Numerical Study of the Fabrication Tolerance of Conventional and MMI-Flattened AWGs

Thomas Kamalakis and Thomas Sphicopoulos, *Member, IEEE*

***Abstract*—In this letter, the fabrication tolerance of conventional and multimode interference (MMI)-flattened arrayed waveguide gratings (AWGs) is compared. It is shown that the crosstalk of an MMI-flattened AWG is approximately equal to that of a conventional AWG with the same 3-dB bandwidth. However, the dispersion of the MMI-flattened AWG is greater than that of the conventional one and this poses limitations in the maximum bit rate in a cascade of MMI-flattened AWGs.**

***Index Terms*—Crosstalk, gratings, integrated optics, optical filters, tolerance analysis, waveguide filters.**

I. Introduction

ARRAYED waveguide gratings (AWGs) are being used in a variety of applications such as wavelength multiplexers–demultiplexers, multiwavelength receivers, and add–drop multiplexers [1]. The passband of conventional AWGs is inherently Gaussian and this limits the maximum allowable number of devices in an AWG cascade. The number of allowed devices can be increased, using passband flattening techniques. One such technique uses multimode interference (MMI) couplers at the input waveguides [2]. This technique uses a single AWG but results in some loss of diffraction efficiency at the main lobe.

The crosstalk level of AWGs depends on the quality of the fabrication process and on the device size and specifications (channel spacing, number of channels, etc.). Crosstalk levels range from -40 to -30 dB for silica based devices but can be as high as -20 dB for semiconductor-based devices [4]. The crosstalk is mainly due to the phase errors [5], [13] caused by waveguide fabrication imperfections. Coupling in the grating arms can also increase the crosstalk. However, the AWGs are designed so that, in the absence of fabrication imperfections, the coupling-induced crosstalk is less than -40 dB [1] and fabrication imperfections do not cause additional crosstalk deterioration through coupling [5]. Hence, in this letter, where the impact of fabrication imperfections is considered, the effect of coupling is neglected. Using numerical simulations and theoretical considerations, the crosstalk levels of conventional and MMI-flattened AWGs are compared. The phase errors can also induce a group velocity dispersion (GVD) delay in the AWG response. Using numerical and analytical methods, the GVD is shown to be higher in MMI-flattened AWGs than in their conventional counterparts. The limitations of the GVD on the allowable bit rate in an AWG cascade are also addressed.

Manuscript received January 9, 2004; revised April 5, 2004.

The authors are with the Department of Informatics and Telecommunications, University of Athens, GR-15784 Athens, Greece (e-mail: thkam@di.uoa.gr).

Digital Object Identifier 10.1109/LPT.2004.829763

The transfer function $H(v)$ between the central input and output port is given by [6]

$$H(v) = \sum_{m=-P}^{m=P} C_m \exp(j\delta_m + j2\pi m v) \tag{1}$$

where $M = 2P + 1$ is the number of grating arms, C_m is the fraction of the total power intercepted by the mth grating arm, $v = (f - f_0)/\mathrm{FSR}$ is the normalized baseband frequency, f the optical frequency measured in terahertz, f_0 the central frequency of the AWG, and δ_m the phase errors. The distribution C_m is related to the Fourier transform of the fundamental modes of the input and output waveguides. For a conventional AWG, where these modes are approximately Gaussian, C_m is also Gaussian, i.e., $C_m \sim \exp(-am^2)$, where a is related to the 3-dB bandwidth B_c of $H(v)$ through $B_c \cong 0.187a^{1/2}$. In the case of an MMI-flattened AWG, with MMI length L equal to $3L_\pi/8$ (L_π is the beat length of the MMI), the transfer function is a sum of two displaced conventional transfer functions $H_1 = H(v - b/2)$ and $H_2 = H(v + b/2)$. Hence, $C_m \sim \exp(-am^2)\cos(\pi bm)$, where b is the normalized (dimensionless) spectral separation of H_1 and H_2. This C_m distribution arises in other flattening methods in which the transfer function is a sum of two displaced conventional transfer functions such as [7] and [8] and the results of this work hold in these cases as well. For the transverse-electric modes, L_π is given by $L_\pi = 4n_r^2 W_e^2 f/(3c)$ [3], where $W_e = W + c/\pi/f/(n_r^2 - n_c^2)^{1/2}$ the effective mode width, W the actual MMI width, n_r and n_c the core and cladding refractive indexes. Assuming $W = 11\ \mu$m, $n_c = 1.46, n_r = 1.4675$ [3], $f_0 = 193$ THz, and FSR $= 1$ THz, the relative change $\Delta L_\pi/L_\pi$ in L_π at the edges $f = f_0 \pm \mathrm{FSR}/2$ of the FSR is $<1\%$. Hence, $L \cong 3L_\pi/8$ and $C_m \sim \exp(-am^2)\cos(\pi bm)$ at the edge channels as well.

The standard deviation of the phase errors, $\sigma_m^2 = \langle \delta_m^2 \rangle$ was experimentally shown to be proportional to L_m^2, where L_m is the length of the mth grating arm [9]. In most AWGs, the lengths L_m do not vary significantly and σ_m can be taken approximately constant ($\sigma_m \cong \sigma$) [10]. The phase errors are also slightly correlated. This correlation depends on the fabrication process and is difficult to estimate experimentally [10]. In this letter, the phase errors are assumed uncorrelated but the results can be extended to include the phase error correlation, once it is measured experimentally.

II. Crosstalk Analysis

Assuming that the δ_ms are Gaussian distributed, the mean value of the transmittance $T(v) = |H(v)|^2$ is given by [6]

$$\langle T(v) \rangle = \left(1 - e^{-\sigma^2}\right) \sum_{m=-P}^{P} C_m^2 + e^{-\sigma^2} T_i(v) \tag{2}$$

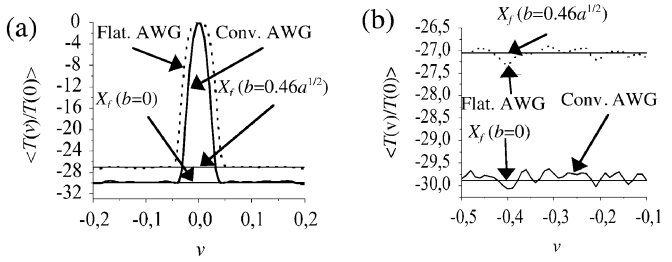

Fig. 1. Numerically estimated $\langle T(v)/T(0)\rangle$ for a flattened (dashed lines) and a conventional AWG (solid lines) (a) near the passband and (b) far from the passband for $M = 75$ and $\sigma = 0.217$. Also shown are the values of X_f obtained from (3).

where $T_i = |H_i(v)|^2$ is the transmittance of an ideal AWG without phase errors ($\delta_m = 0$). Equation (2) still applies to a variety of other passband flattening methods, once the distribution C_m is determined. Outside the main lobe, $T_i(v)$ is very low and $\langle T(v)\rangle$ is determined by the first term only. In the case of an MMI AWG, one can approximate $\sum C_m^2$ (2) by $\int_{-\infty}^{+\infty} \exp(-2am^2)\cos^2(\pi bm)\,dm$, which is known in closed form [11, eq. (3.898.2)]. In a similar way $\langle T(0)\rangle$ can be approximated in closed form using [11, eq. (3.896.1)], and the mean crosstalk level $X = \langle T(v)\rangle/\langle T(0)\rangle$ where v is outside the main lobe, is written as

$$X_f \cong \left(e^{\sigma^2} - 1\right)(a/8/\pi)^{1/2}\left(e^{\pi^2 b^2/a/2} + 1\right). \qquad (3)$$

Equation (3) gives the mean crosstalk level of an MMI flattened AWG when $L = (3/8)L_\pi$. For $L \neq (3/8)L_\pi$, the distribution of C_m must be evaluated from the incident field at the output of the MMI [3] and X_f can be computed in a similar way. The mean crosstalk level X_c of a conventional AWG is obtained from (3) setting $b = 0$. The validity of (3) is shown in Fig. 1, where the average $T(v)/T(0)$, calculated using 1000 randomly generated transfer function samples, is plotted both with dashed lines for Fig. 1(a) an MMI flattened and Fig. 1(b) a conventional AWG for $\sigma = 0.217$. The value of σ is chosen so that the expected value of X in the case of a conventional is $\cong -30$ dB. Also plotted with a solid line is the mean crosstalk level estimated from (3). The value of b in the case of the flattened AWG was taken $b = 0.46a^{1/2}$, which ensured a flat passband with low ripple. The 3-dB bandwidth of the conventional AWG is $B_c = 0.02$ and the number of waveguides used is $M = \lceil 4/a^{1/2}\rceil = 75$ which ensured a power truncation of less than 1% in the grating waveguides. The number of waveguides of the flattened design is also $M = 75$ and its 3-dB bandwidth is $B_f = 0.38a^{1/2} \cong 0.046$. As seen in Fig. 1, (3) provides an accurate estimation of the mean crosstalk level for both types of AWGs.

The AWGs compared in Fig. 1 have the same number of waveguides and, hence, the same a. Using (3), the crosstalk ratio X_f/X_c of the conventional and the flattened AWG equals $X_f/X_c = (\exp(\pi^2 b^2/2/a) + 1)/2 \cong 1.92 \cong 2.8$ dB (independent of σ). Hence, an MMI-flattened AWG has about 3-dB higher crosstalk compared to a conventional AWG with the same number of waveguides. Note that a different value of b does not significantly alter this conclusion. If b is increased by 10%, the change in the ratio X_f/X_c is less than 0.2 dB. This 3-dB crosstalk deterioration is partially due to the reduction of the diffraction efficiency at the main lobe induced by the passband flattening. This lowers the peak of the main lobe by about -2.1 dB [3]. An additional deterioration ($\cong -0.7$ dB) is due to the change of the coefficients C_m.

If the value a_f of a of the flattened AWG is chosen $a_f = 0.242a$, then its 3-dB bandwidth $B_f = 0.38a_f^{1/2}$ equals that of the conventional AWG $B_c = 0.187a^{1/2}$, and using (3), the ratio X_f/X_c is $X_f/X_c \cong 0.93$. Hence, if both types of AWG have the same bandwidth, their crosstalk levels are approximately equal.

III. Dispersion Characteristics

To analyze the dispersion characteristics of AWGs, the phase $\phi(v)$ of $H(v)$ must be considered. If R and V are the real and imaginary parts of $H(v)$, then $\phi(v) = \tan^{-1}(V/R)$. Assuming that the δ_ms are small, then $\exp(j\delta_m) \cong 1 + j\delta_m$ and R and V are approximated by $\sum C_m \cos(2\pi mv) \cong H_i(v)$ and $\sum C_m\delta_m \sin(2\pi mv) + \sum C_m \sin(2\pi mv)$. Since C_m is symmetric and $\sin(2\pi mv)$ antisymmetric with respect to m, one has $\sum C_m \sin(2\pi mv) = 0$ for $v \neq 0$ and, hence, $V \cong \sum C_m\delta_m \sin(2\pi mv)$. The GVD $\phi_2 = \phi''(v)$ is given by the second derivative of ϕ'. Using the fact that the phase variation within the passband is small (in which case $V/R = \tan^{-1}\phi \cong \phi$), one can prove that for small δ_m

$$\phi_2(v) = \sum_m D_m(v)\delta_m \qquad (4)$$

where

$$D_m(v) = \left(A(v) - t_m^2 C(v)\right)\cos(t_m v) - t_m B(v)\sin(t_m v) \qquad (5)$$

$$A(v) = H_i'^2/H_i^3 - H_i''/H_i^2 \qquad (6a)$$

$$B(v) = -2H'_i/H_i \qquad (6b)$$

$$C(v) = H_i^{-1} \qquad (6c)$$

with $t_m = 2\pi m$ and H_i the ideal transfer function ($\delta_m = 0$). Squaring (4) and taking its expected value, one can derive the standard deviation $\sigma_2(v)$ of the GVD

$$\sigma_2^2(v) = \langle \phi_2^2(v)\rangle = \sigma^2 \sum_m D_m^2(v). \qquad (7)$$

The validity of (7) is shown in Fig. 2, where $\sigma_2(v)$ is plotted for $\sigma = 0.217$ in the case of Fig. 2(a) a flattened AWG with $B' = 0.042, M = 75$, Fig. 2(b) a conventional AWG with $B = 0.02, M = 75$, and Fig. 2(c) a flattened AWG with $B' = 0.02, M = 155$. The solid lines are computed using (7) while the dots are numerically computed from the phase response $\phi(v)$ of 1000 randomly generated transfer functions. As shown in Fig. 2, (7) adequately describes $\sigma_2(v)$ in all three cases. The conventional AWG has higher GVD than the flattened AWG with the same number of waveguides. However, the GVD of the conventional AWG is lower than that of the flattened AWG with the same 3-dB bandwidth. In Fig. 3(a), the value of $\sigma_2(0)/\sigma$ of the conventional (solid line) and the flattened AWG (dashed line) are plotted as a function of the 3-dB bandwidth. The ratio of $\sigma_2(0)$ of the conventional and the flattened AWG is approximately constant and equal to 0.48 implying that the standard deviation of the GVD at the central frequency is about

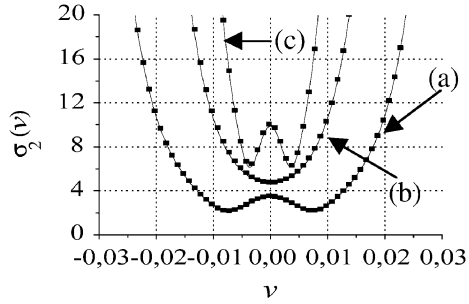

Fig. 2. Value of $\sigma_2(v)$ computed from (7) (solid lines) and from numerical simulations (dots) for $\sigma = 0.217$ and (a) a flattened AWG with $B = 0.046$, (b) a conventional, and (c) a flattened AWG with $B = 0.02$.

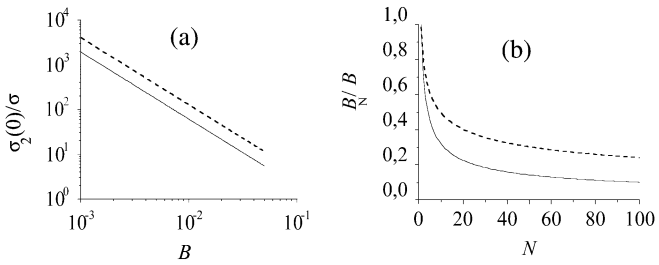

Fig. 3. (a) GVD at the center of the transfer function $\sigma_2(0)/\sigma$ in the case of a conventional (solid line) and a flattened (dashed line) as a function of the 3-dB bandwidth B and (b) the 3-dB bandwidth B_N of a cascade of N AWGs divided by the 3-dB bandwidth of each device in the cascade in the case of conventional (solid lines) and MMI-flattened devices (dashed lines).

50% higher for MMI-flattened AWGs with the same 3-dB bandwidth (regardless of σ).

The total GVD delay in a cascade of aligned AWG devices of equal 3-dB bandwidth will be given by the sum of the GVD delays of each device in the cascade. Assume a cascade of $N = 100$ devices with FSR $= 1$ THz and let the 3-dB bandwidth of the transfer function of the entire cascade be equal to 10 GHz (implying a normalized value $B_N = 0.01$). The 3-dB bandwidth of each device B is calculated using Fig. 3(b), the value of B_N/B both for flattened (solid line, $B = B_f$) and conventional devices (dashed lines, $B = B_c$). Using Fig. 3(a), it is deduced that the normalized 3-dB bandwidth of each AWG must be equal to $B_c = 0.1$ (100 GHz) for the conventional AWG and $B_f \cong 0.04$ (40 GHz) for the flattened AWG. The value of $\sigma_2(0)/\sigma$ obtained are 1.9 and 16.1 respectively. Assuming that $\sigma = 0.217$, one has $\sigma_2(0) = 0.42$ and $\sigma_2(0) = 3.51$, respectively. Assuming that N is large, the total GVD delay can be assumed Gaussian with standard deviation $\sigma_{\rm tot}$ (measured in picoseconds) equal to $\sigma_{\rm tot} = N^{1/2}\sigma_2(0)\mathrm{FSR}$ which corresponds to 4.2 ps for the conventional and 35.1 ps for the flattened AWG cascade. In order to ensure less than 1-dB power penalty, the GVD delay must not exceed 30% of the bit duration $1/R_b$ (where R_b is the bit rate) [12] and, hence, $0.3/R_b < 3\sigma_{\rm tot}$, since a Gaussian random variable of variance $\sigma_{\rm tot}$ can be assumed contained in $[-3\sigma_{\rm tot}, 3\sigma_{\rm tot}]$. The maximum bit rate $R_{\max}$ is 3.2 Gb/s for the flattened devices and 23.8 Gb/s for the conventional ones. These rate limits are posed by the GVD alone and one should take into account other factors as well. In the case of the conventional AWGs, it is obvious that the 23.8-Gb/s rate limit is unachievable because the 3-dB bandwidth of the cascade is 10 GHz, which cannot accommodate such a high bit rate. Also, since B_f is much smaller than B_c, more wavelength channels can be supported in the flattened cascade. Nevertheless, the above calculations imply that the GVD may become a problem for a cascade of MMI-flattened devices.

IV. Conclusion

In this letter, the fabrication tolerance of conventional and MMI-flattened AWGs was compared both theoretically and numerically. It was shown that the crosstalk of an MMI-flattened AWG is approximately equal to that of a conventional AWG with the same 3-dB bandwidth. The AWG GVD delay and its implications in an AWG cascade were also considered. It was deduced that the GVD can pose important limitations in an cascade of MMI-flattened AWGs.

References

[1] M. K. Smit and C. Dam, "PHASAR-based WDM-devices: Principles and applications," *IEEE J. Select. Topics Quantum Electron.*, vol. 2, pp. 236–250, June 1996.

[2] M. R. Amersfoort, J. B. D. Soole, H. P. LeBlance, N. C. Andreadakis, A. Rajhel, and C. Caneau, "Passband broadening of integrated arrayed waveguide filters using multimode interference couplers," *Electron. Lett.*, vol. 23, pp. 449–451, 1996.

[3] D. Dai, S. Liu, S. He, and Q. Zhou, "Optimal design of an MMI coupler for broadening the spectral response of an AWG demultiplexer," *J. Ligthwave Technol.*, vol. 20, pp. 1597–1961, Nov. 2002.

[4] Y. Yoshikuni, "Semiconductor arrayed waveguide gratings for photonic integrated devices," *IEEE J. Select. Topics Quantum Electron.*, vol. 8, pp. 1102–1114, Nov./Dec. 2002.

[5] C. Dragone, "Crosstalk caused by fabrication errors in a generalized Mach-Zehnder interferometer," *Electron. Lett.*, vol. 33, pp. 1326–1327, July 1997.

[6] T. Kamalakis, T. Sphicopoulos, and D. Syvridis, "An estimation of performance degradation due to fabrication errors in AWGs," *IEEE J. Lightwave Technol.*, vol. 20, pp. 1779–1787, Sept. 2002.

[7] Y. P. Ho, H. Li, and Y. Chen, "Flat channel passband wavelength multiplexing and demultiplexing devices by multiple Rowland circle design," *IEEE Photon. Technol. Lett.*, vol. 9, pp. 342–344, Mar. 1997.

[8] M. R. Amersooft *et al.*, "Phased-array wavelength demultiplexer with flattened wavelength response," *Electron. Lett.*, vol. 30, no. 4, pp. 300–301, Feb. 1994.

[9] T. Goh, S. Suzuki, and A. Sugita, "Estimation of waveguide phase error in silica-based waveguides," *J. Lightwave Technol.*, vol. 15, pp. 2107–2113, Nov. 1997.

[10] K. Maru, M. Okawa, K. Matsui, and H. Uetsuka, "Statistical analysis of correlated phase error in transmission characteristics of arrayed-waveguide gratings," *IEEE J. Select. Topics Quantum Electron.*, vol. 8, pp. 1142–1148, Nov./Dec. 2002.

[11] I. S. Gradshteyn and I. M. Ryzhik, *Table of Integrals Series and Products*, 6th ed. New York: Academic, 1980.

[12] R. Ramaswami and K. N. Sivarajan, *Optical Networks: A Practical Perspective*. San Mateo, CA: Morgan Kaufman, 1998.

[13] K. Takada, H. Yamada, and Y. Inoue, "Origin of channel crosstalk in 100 GHz-spaced silica-based arrayed-waveguide grating multiplexer," *Electron. Lett.*, vol. 31, no. 14, pp. 1176–1178, July 1995.